MeV range particle physics studies in tokamak plasmas using gamma-ray spectroscopy

M. Nocente[1,2], A. Dal Molin[1], N. Eidietis[3], L. Giacomelli[2], G. Gorini[1,2], Y. Kazakov[4], E. Khilkevitch[5], V. Kiptily[6], M. Iliasova[5], A. Lvovskiy[7], M. Mantsinen[8], A. Mariani[2], E. Panontin[1], G. Papp[9], G. Pautasso[9], C. Paz-Soldan[3], D. Rigamonti[2], M. Salewski[10], A. Shevelev[5], M. Tardocchi[2] and JET‡ and MST1§ contributors

[1] Dipartimento di Fisica "G. Occhialini", Università di Milano-Bicocca, Milano, Italy

E-mail: massimo.nocente@mib.infn.it

[2] Istituto per la Scienza e Tecnologia dei Plasmi, Consiglio Nazionale delle Ricerche, Milano, Italy

[3] General Atomics, San Diego, USA

[4] Laboratory for Plasma Physics, Brussels, Belgium

[5] Ioffe Institute, St. Petersburg, Russia

[6] Culham Centre for Fusion Energy, Culham, United Kingdom

[7] Oak Ridge Associated Universities, Oak Ridge, USA

[8] Barcelona Supercomputing Centre and ICREA, Barcelona, Spain

[9] Max Planck Institute for Plasma Physics, Garching, Germany

[10] Technical University of Denmark, Kgs. Lyngby, Denmark

12th July 2019

Abstract.

Gamma-ray spectroscopy (GRS) has become an established technique to determine properties of the distribution function of the energetic particles in the MeV range, which are fast ions from heating and fusion reactions or runaway electrons born in disruptions.

In this paper we present a selection of recent results where GRS is key to investigate the physics of MeV range particles. These range from radio-frequency heating experiments, where theoretical models can be tested with an unprecedented degree of accuracy, to disruption mitigation studies, where GRS sheds light on the effect of the actuators on the runaway electron velocity space.

We further discuss the unique observational capabilities offered by the technique in deuterium-tritium plasmas, particularly with regard to the inference of the energy- and pitch-resolved distribution function of the α particles born from fusion reactions in the plasma core.

‡ See the author list of E. Joffrin et al. accepted for publication in Nuclear Fusion Special issue 2019, https://doi.org/10.1088/1741-4326/ab2276

§ See author list of B. Labit et al 2019 Nucl. Fusion accepted (doi:10.1088/1741-4326/ab2211)

Keywords: Gamma-ray spectroscopy, Fast particles, Nuclear fusion

1. Introduction

Energetic particles, ions as well as electrons, are ubiquitous in tokamaks. They are generated by heating systems, that rely on the injection of neutral beams (NBI) [1, 2] or radio frequency (RF) waves [3, 4] to reach core temperatures of some keV required by the fusion process. Each type of heating mechanism is a source of energetic ions, often in the MeV range, that must be confined until they transfer their energy to the bulk plasma by Coulomb collisions. Another prominent source of MeV range ions are the fusion reactions [5, 6], particularly alpha particles in plasmas of deuterium-tritium (DT), as they provide the self-heating mechanism that is essential for the sustainment of the fusion burn.

While ensuring good plasma confinement by the magnetic fields is one of the aims of tokamak research, sometimes the equilibrium is suddenly lost, and the plasma disrupts. In these scenarios, significant electric fields are induced, and they can accelerate thermal electrons up to energies of tens of MeV. These so-called "runaway" electrons (REs)[7, 8] experience a decreasing Coulomb friction as they gain energy from the electric fields, until there is a balance between the generation and dissipation mechanisms (radiation emission and losses to the first wall). If the fraction of the initial plasma current that is turned into a RE beam is significant, there is a potential risk for the integrity of the machine by the impact of the REs on the first wall. This has lead to the worldwide development of avoidance and mitigation techniques.

In both heating and disruption scenarios, there is need to measure the distribution function of the energetic, confined particles, as this reflects the effects of the actuators (intrinsic/extrinsic heating or mitigation and avoidance techniques for REs) on the plasma. At the same time, however, this measurement is not straightforward to obtain and only few indirect methods can be adopted.

Gamma-ray spectroscopy (GRS) is one of the few experimental techniques that bring information on fast ions (FI) and REs. FI measurements by GRS are based on spontaneous nuclear reactions between the FIs and naturally occurring impurities [9, 10, 11]. These lead to the production of a heavy nucleus in an excited state that, when it de-excites, results in the emission of discrete gamma-ray quanta (lines), whose energy is determined by each specific nuclear reaction. As most of the FI in the MeV range lead to nuclear reactions, a single gamma-ray spectrum from a tokamak plasma is a diagnostics of different FI species simultaneously, and the number, intensity and shape of the lines embeds information on their distribution functions.

MeV range REs are instead manifested by the bremsstrahlung radiation they emit as they collide with the plasma ions or impurities [12, 13]. Unlike the case of FI driven reactions, the MeV range energy spectrum of this so called hard x-ray (HXR) emission is continuous and there is interest in measuring its shape and spatio-temporal evolution, which again depends on the distribution function of the REs. In this application, an

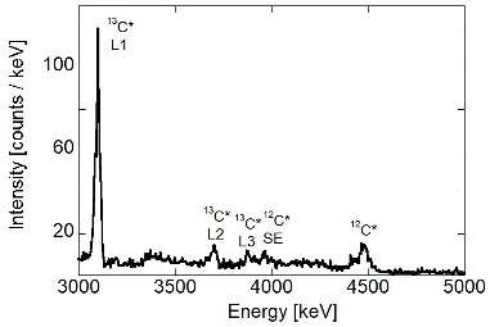

Figure 1. Gamma-ray spectrum from a JET ^{4}He plasma with third harmonic ICRH acceleration of a ^{4}He beam. Lines from the ^{12}C(d, pγ)^{13}C and ^{9}Be(α, nγ)^{12}C reactions, leading to gamma-rays at different energies in the range E_γ=3 to 5 MeV are clearly visible and are indicated by the excited nucleus they lead to. SE indicates the single escape peak of the E_γ =4.44 MeV line and is a feature of the instrument used to carry out the measurements. Figure reproduced with permission from [22]

additional difficulty comes from the fast time scales of a disruption, which ranges from few milliseconds to tens of milliseconds. This dictates the use of spectrometers with MHz counting rate capabilities [14, 15, 16, 17].

In this paper, we present examples of physics studies using GRS both in FI and RE experiments in large as well as mid-size devices. GRS determines the FI distribution function predominantly in experiments on ion cyclotron resonance heating (ICRH) by the RF waves that provide a source of energetic ions as a way to study aspects of their physics. In disruption studies, GRS captures the time evolution of the maximum RE energy, which responds differently to the actuators. We finally address the prospects of GRS in view of alpha particle measurements in DT plasmas, both in the forthcoming JET campaign [18] and at ITER [19, 20], in particular in relation with the possibility to infer the energy- and pitch-resolved alpha particle distribution function by means of velocity space tomography [21].

In the text that follows, in order to focus on the plasma physics aspects that gamma-ray spectroscopy can investigate, we have deliberately decided not to mention the many detector subtleties behind the measurements. The reader who is interested in the instrumental facets of this field is referred to the recent comprehensive review [11].

2. Fast ion studies using gamma-ray spectroscopy

In FI experiments, the relatively large number of nuclear reactions between the FI and the impurities often leads to a complex gamma-ray spectrum. An example is shown in figure 1, which shows data from a JET experiment [22] aimed at generating MeV range ^{4}He ions in a ^{4}He plasma by coupling RF waves on to a ^{4}He beam using ICRH at the third harmonic [23]. Besides ^{4}He, in this scenario we also expect to accelerate deuterons, which share the same charge to mass ratio as ^{4}He and were present in the plasma at trace levels from previous deuterium operations. This is confirmed by the gamma-ray

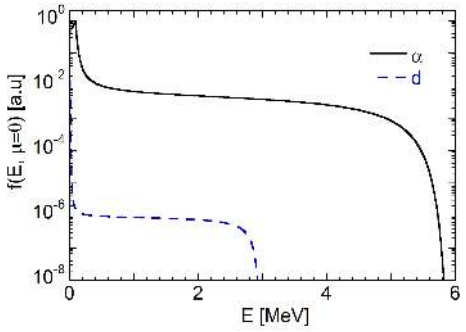

Figure 2. Expected energy distribution function of deuterons and α particles accelerated by RF waves at the third ion cyclotron harmonic, based on the one-dimensional extended Stix model of [22] and at a pitch $\mu = 0$. Figure reproduced with permission from [22]

spectrum, that shows lines from the $^{12}\mathrm{C}(\mathrm{d},\mathrm{p}\gamma)^{13}\mathrm{C}$ and $^{9}\mathrm{Be}(\alpha,\mathrm{n}\gamma)^{12}\mathrm{C}$ reactions. Here ^{12}C comes from the JET carbon wall installed at the time of the experiment. In this scenario, theory predicts a highly non Maxwellian shape for the FI distribution function (see figure 2), with a sharp cut-off at an energy E^*.

A simplified, analytical model of the distribution function can be set up in this case [22] and depends on two free parameters. These are the perpendicular component of the wave vector, k_P, and the coupled RF power density P_{RF}, which have to be determined from measured data. A synthetic diagnostic framework is set up so that, given a choice of the k_P and P_{RF} parameters, we are able to calculate the shape and intensity of a particular gamma-ray line through a Monte Carlo method [24] and for comparison with data. A first parameter of interest is here the ratio of the intensities Y_γ of the peaks at E_γ=3.09 and 3.68 MeV from the first (L1) and second (L2) excited states of ^{12}C born from the $^{12}\mathrm{C}(\mathrm{d},\mathrm{p}\gamma)^{13}\mathrm{C}$ reaction, as it can be used to constrain the FI distribution function in this scenario. This is shown in figure 3, where the measured ratio with error bar (gray stripe) is compared with the Monte Carlo calculation of the expected ratio starting from the analytical distribution function described above and for the different k_P and P_{RF} parameters as input. We observe that the calculated ratio is almost insensitive to P_{RF}, but it changes depending on k_P and we can use this to find which k_P interval yields intensity ratios that fall within the experimental grey stripe of figure 3. As k_P in turn determines the cut-off energy, we obtain E_d^* in the range 3.0 ± 0.2 MeV.

Data from the same experiment also offer the possibility to determine E_α^* and to verify the expected relation $E_\alpha^* = 2 \times E_d^*$. This is obtained by using the Monte Carlo framework introduced above to predict the shape of the $^{9}\mathrm{Be}(\alpha,\mathrm{n}\gamma)^{12}\mathrm{C}$ peak at E_γ=4.44 MeV and shown in figure 4. Again, the framework yields different shapes depending on the input k_P, but there is one that best fits the data and corresponds to the blue curve of figure 4. From this we find $\mathrm{k_P} \approx 45\ \mathrm{m}^{-1}$, that translates into $E_\alpha^* \approx$6 MeV which, as expected, is twice the deuterium cut-off energy.

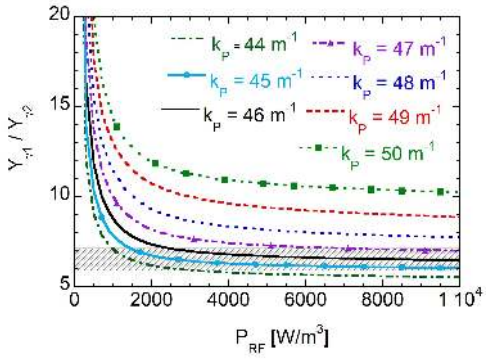

Figure 3. Ratio between the intensity Y_γ of the gamma-ray emission from the first and second excited states of ^{13}C born from the ^{12}C(d, pγ)^{13}C reaction as a function of the k_P and P_{RF} parameters that define the shape of the deuteron distribution function.

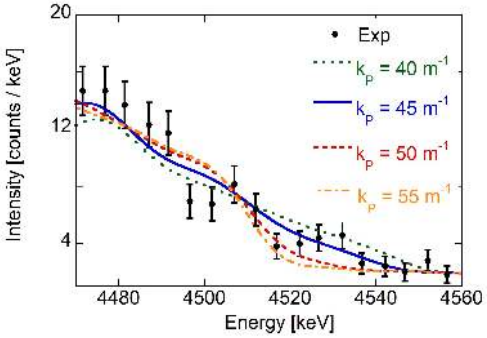

Figure 4. High energy tail of the E_γ=4.44 MeV peak from the ^{9}Be(α, nγ)^{12}C reaction. The lines are fits of the experimental data starting from a model of the alpha particle distribution function where the cut-off energy E^* is modified by changes of the k_P parameter. The solid line shows the best fit to the data, which is obtained when $k_P = 45\ m^{-1}$, corresponding to $E^* = 6$ MeV. Figure reproduced with permission from [22].

A more recent example where GRS is key to study FI physics comes from experiments aimed at testing the novel, so-called three-ion ICRH scheme [25, 26]. In this scenario, a minority population at typical concentrations of few percents or less is heated by RF waves in a plasma of two majority species, for example ^{3}He as the minority in a plasma of hydrogen and deuterium (H-(^{3}He)-D). The concentration of the two majorities is carefully chosen so that the left cut-off layer of the incoming wave coincides with the absorption layer of the minority species. In this way, the polarization of the wave electric field at the resonance is fully left handed and a virtually 100% absorption of the wave power is possible.

A first experiment on the H-(^{3}He)-D three ion scenario has been recently performed at JET. For this case, RF simulations with the PION code [27](see figure 5 left) predict that the tail temperature of the FI must exceed 1 MeV in the plasma core, where the left cut-off layer is found when the H:D concentrations are in the ratio of about 70:30.

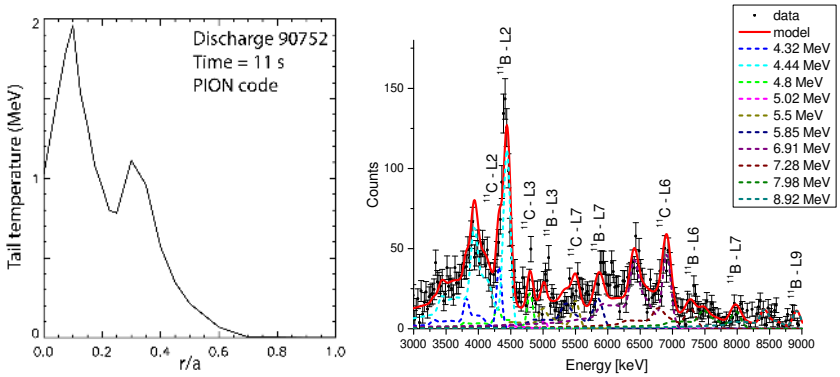

Figure 5. (left) PION calculation of the tail temperature of the ^{3}He ions at different positions in the plasma cross section for the three-ion H-(^{3}He)-D scheme and as a function of the normalized poloidal radius r/a. (right) Gamma-ray spectrum observed by a vertical spectrometer in the same scenario. The emission is interpreted in terms of the contributions from the ^{9}Be(^{3}He, pγ)^{11}B and ^{9}Be(^{3}He, nγ)^{11}C reactions using the response function of the instrument. Lines are marked by the excited nucleus they come from.

The experimental confirmation of this is given by GRS, which observes a rich spectrum made of lines from the de-excitation of several excited states of ^{11}B and ^{11}C nuclei born in the ^{9}Be(^{3}He, pγ)^{11}B and ^{9}Be(^{3}He, nγ)^{11}C reactions (figure 5 right).A model of the response function of the specific instrument used for GRS (a $LaBr_3$ detector in this case [28]) can be used to resolve the individual emissions and to identify their intensities. As for the ^{4}He case, we can set up a Monte Carlo model where the PION distribution function is used as input to calculate the expected intensities and shapes of the lines observed for comparison with data. A preliminary analysis along this line is reported in [29], where the main difficult here is related to the availability of good cross section data for ^{3}He induced gamma-ray reactions, which limits the exploitability of the spectrum to a few lines at the moment. Still, at least qualitatively, the Monte Carlo framework confirms that ions to the MeV range must have been generated in the plasma and in agreement with the PION results. Otherwise, many of the observed lines would not be measured according to calculations.

Another opportunity provided by GRS is the possibility to make spatially resolved images of the gamma-ray emission, which is obtained by observing the plasma along multiple lines of sight at the same time [18, 30, 10]. This is useful to tell the FI profile in the poloidal cross section and to observe how this changes in response to the external actuators. An example from the H-(^{3}He)-D scenario is shown in figure 6, where the emission from ^{3}He induced reactions is compared when the dominant wave number of the launched wave spectrum is changed. In this case, theory predicts a different FI profile, which is more core localized when the antennas are operated in the so called $\pi/2$ phasing, as observed (see [26] for details).

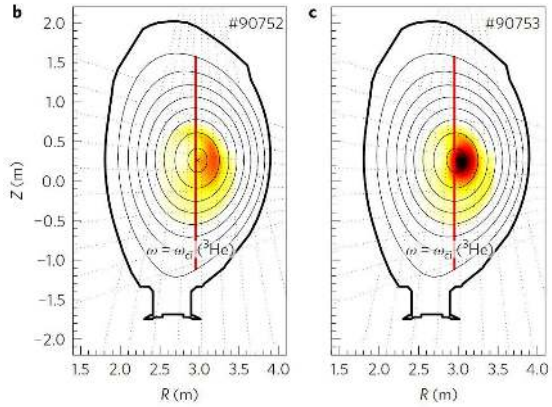

Figure 6. Spatial maps of the gamma-ray emission in the poloidal cross section for the H-(^{3}He)-D three ion scenario. In the two discharges, the same RF power is delivered by using different phasings for the antenna, which results in a different wave number spectrum. More core localized emission is observed for the figure to the right, where part of the RF power is provided using the $\pi/2$ phasing. Figure reproduced with permission from [26].

3. Runaway electron studies using gamma-ray spectroscopy

The mitigation of REs born in disruptions is one of the priorities in view of ITER [31]. The concern is that a localized loss of the RE beam may damage the tokamak first wall, which is a major risk for plasma operations. Mitigation techniques, predominantly based on massive gas injection (MGI) or shattered pellet injection (SPI) have been developed and are being tested on mid and large-scale tokamaks worldwide [32, 33, 34] with the aim of preventing the development of a large RE current which would be unbearable for the integrity of the device. In this context, GRS measurements of the HXR bremsstrahlung spectrum born from the REs are key, as they provide access to the RE distribution function and how it responds to the external actuators. This is of relevance to validate models of the RE physics, which is deemed necessary to increase confidence in view of their use for ITER.

The relation between the HXR spectrum S and the RE distribution function F is however indirect and is mediated by a weighting matrix W. The latter can be rather complex to evaluate, as it embeds information on the bremsstrahlung generation process, radiation transport from the plasma to the detector, the line of sight of the device and the way the instrument responds to impinging gamma-rays of different energies. On the other hand, once W is known, the mathematical relation between S and F is formally simple and, in matrix form, it reads as $S = WF$. Here S and F are discrete representations of the HXR spectrum and the RE distribution function, respectively. If a model for F is known, the expected spectrum S can be readily evaluated by matrix multiplication and can be compared to the actual, measured spectrum for validation. In most cases, however, the complexity of the problem, where a large number of plasma parameters varies by orders of magnitude over the time scale of few ms, makes a calculation of F extremely

challenging. In common applications, one has thus to infer F from S without a prior model, which is mathematically an ill-posed problem. Different inversion methods [35, 36] are used for this application and provide F with some systematic uncertainties. The methods deconvolve F from S by making hypotheses on some features of the solution, for example the fact that F must be non negative and a sufficiently smooth function [21]. One of the most popular method is that due to Tikhonov, but many others have been used and are often borrowed from the more traditional field of real space tomography, for example those used in Positron Emission Tomography applications.

Figure 7 left shows an example of deconvolution of the RE distribution function in an experiment at the ASDEX Upgrade tokamak, where the HXR spectrum is measured along a collimated radial sight-line and during a disruption triggered by Argon injection at 1 s. The RE beam is let to evolve without further external intervention, until it completely dissipates in about 1.5 s from its generation. The corresponding RE distribution functions obtained by deconvolution of the data are shown to the right and, besides some oscillations that are likely artefacts of the inversion method, they clearly indicate a reduction of the maximum RE energy $\mathrm{E_{max}}$ as the beam evolves.

Information on the RE distribution function, even if limited, is particularly valuable as it sheds further light on the physics behind a disruption. One of the most recent examples comes from a DIII-D experiment [37], where kinetic instabilities driven by the REs during the current quench were observed for the first time. GRS measurements of the HXR emission from the plasma core made it possible to determine $\mathrm{E_{max}}$ with a time resolution better than 1 ms and to understand some of the experimental conditions that triggered the instabilities. Figure 8 top shows a magnetic spectrogram from two of the DIII-D discharges. The lower spectrogram corresponds to the case when a fully developed RE beam in the current quench is observed, while the upper spectrogram comes from a discharge without the development of a RE beam. When $\mathrm{E_{max}}$ exceeds roughly 2.5 MeV, more intense kinetic instabilities are observed, which prevents the development of a RE beam and increases losses. In the opposite case, the instabilities are weaker or barely observed. This is further confirmed by the analysis of the correlation between $\mathrm{E_{max}}$ and the magnetic field perturbation $\tilde{B}_\phi$ associated to the instabilities. It is seen that $\tilde{B}_\phi$ increases linearly with $\mathrm{E_{max}}$ above about 6 MeV. Under these conditions, no RE plateau is formed in most cases.

4. Prospects for α particle measurements in future JET and ITER deuterium-tritium plasmas

Perhaps the most important application of GRS is the possibility to measure α particles in plasmas with deuterium and tritium mixtures in forthcoming JET and ITER experiments. This is achieved by the $^9\mathrm{Be}(\alpha, \mathrm{n}\gamma)^{12}\mathrm{C}$ reaction [38, 39] that spontaneously occurs between fusion born α particles and ^{9}Be impurities and that leads to the emission of a gamma-ray at the characteristic energy of 4.44 MeV. The most

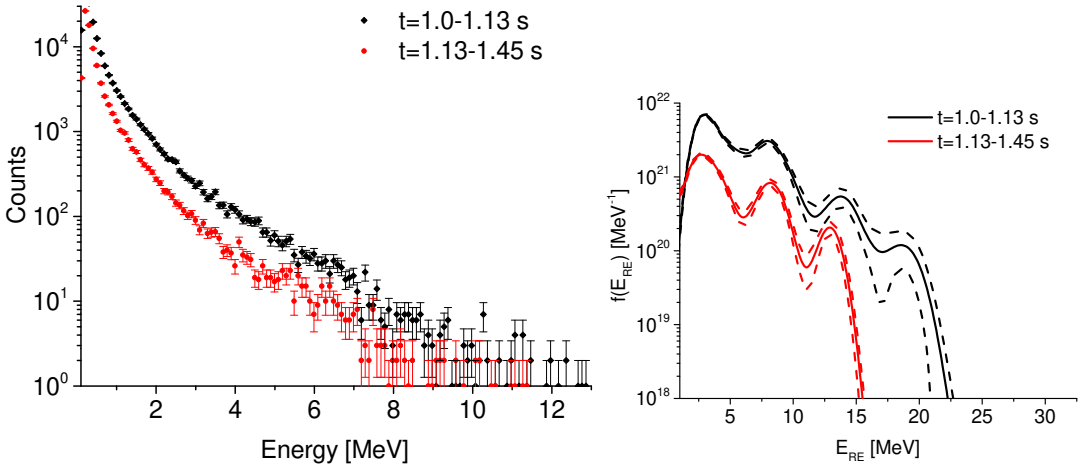

Figure 7. (left) MeV range HXR spectrum from an ASDEX Upgrade discharge where a disruption is triggered by massive Argon injection. (right) RE distribution function obtained by the deconvolution of the data to the left. Figure reproduced with permission from [17].

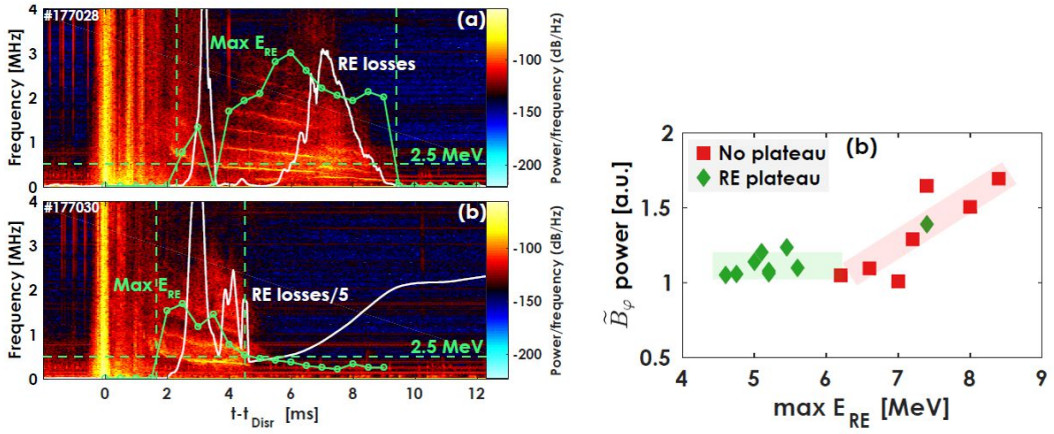

Figure 8. (left) Magnetic spectrogram measured in DIII-D discharges on runaway electron mitigation by massive gas injection. Depending on the maximum RE energy, kinetic instabilities are observed (upper panel) or not (lower panel), which determines the development of a RE beam in the current quench phase of the disruption. (right) Correlation between the amplitude of the kinetic instabilities, the maximum energy of the REs and the existence of a RE beam at the plateau. Figure reproduced with permission from [37].

conceptually straightforward (albeit experimentally challenging) application of GRS consists of multiple sight-line measurements of the 4.44 MeV emission which, similarly to the three ion scheme example discussed above (see section 2), provides the α particle profile in the poloidal cross section [30].

There is however a more challenging (yet highly promising) application of GRS for α particle studies and that comes by the observation of the same plasma volume through lines of sight that make different angles with respect to the magnetic field in that volume.

The technique, known as velocity space tomography (VST) [21, 40, 11], relies on the concept of weight functions (discretized by matrices). These are energy- and pitch resolved functions that tell which region of the fast ion velocity space is represented in a particular spectral measurement such as, for example, a given energy bin of a gamma-ray spectrum. The details of the weight function depend on the physics of the emission process (for example gamma-ray or neutron emission), the angle that the line of sight of the instrument makes with respect to the magnetic field and the particular channel of the spectrum that is selected. Weight functions have been derived for a large number of FI diagnostics [41, 42, 43, 44, 45], including, more recently, GRS [46, 47]. Once these are known, one can formally write the same equation that connects the RE distribution function to the HXR spectrum, $S = WF$ (see section 3), and attempt to find F from S by using inversion methods. In the VST application, S represents the collection of the radiation spectra emitted by the FI (gamma-ray spectra, but also neutron diagnostics, collective Thomson scattering etc.); W comprises all of the weight functions of the diagnostics that are used for the inversion; F is the energy- and pitch resolved FI distribution function that needs to be found.

The power of the technique has been demonstrated predominantly in relation to FI experiments on mid-size devices [21, 48, 49] and, more recently, also in a JET experiment with MeV range deuterons and based on a combination of neutron and gamma-ray measurements [50, 40].

GRS based VST holds promises also for α particle studies, as recently demonstrated in [51]. Figure 9 left shows a calculation of the α particle distribution function for the ITER baseline scenario with the ASCOT code. We assume that the core plasma is viewed with two gamma-ray instruments, one vertical and one tangential, and with an energy resolution that is sufficient to resolve the Doppler broadened shape of the 4.44 MeV peak from the $^9\mathrm{Be}(\alpha, \mathrm{n}\gamma)^{12}\mathrm{C}$ reaction. Assuming the ASCOT calculation as the ground truth (F, in our previous notation), we can evaluate the synthetic GRS signals S that might be measured in this scenario at ITER. As the weight functions for the 4.44 MeV peak are known, we can try to re-obtain F from S using the VST technique. The inferred α particle distribution function F is shown in figure 9 right and closely resembles the ASCOT ground truth, which provides confidence on the applicability of VST for α particle studies by GRS in deuterium-tritium plasmas. Clearly, the actual realization of the technique at ITER and high performance plasmas in general must face a number of experimental challenges, particularly with respect to the capability of extracting the 4.44 MeV signal out of the significant background induced by the interaction of fusion born 14 MeV neutrons with the detector [52, 53]. To this end, forthcoming JET experiments with deuterium-tritium mixtures will represent a unique testbed for this technique, before its application at ITER, and might provide the first experimental visualization of the α particle distribution function in DT plasmas.

2D velocity distribution functions hold all information about energy spectra and fast ion densities, too, such that these quantities can also be obtained. Lastly, it is also possible to obtain alpha particle energy spectra and hence densities from measurements

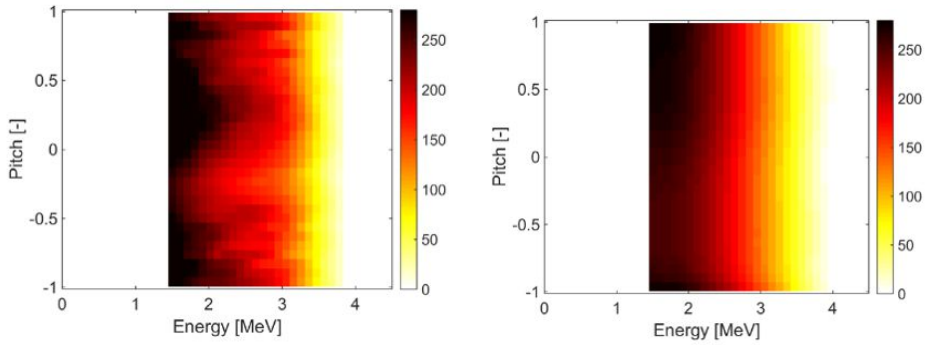

Figure 9. (left) Alpha particle distribution function in the ITER baseline scenario as calculated by the ASCOT code (right) Reconstruction of the distribution function to the left by using velocity space tomography and assuming that measurements are taken with two 90 degree gamma-ray and CTS views, together with a 30 degree gamma-ray view. Figure reproduced with permission from [51].

by solving an easier 1D inversion problem assuming isotropy [54]. This technique allows either inversion of spectra from a single or from several instruments.

5. Conclusions

Gamma-ray spectroscopy (GRS) is a powerful diagnostic for studying fast particles (FI) in tokamak plasmas. In fast ion experiments, GRS observes the line emission from a number of spontaneous nuclear reactions in the plasma and uses those to determine the properties of the FI distribution function. In disruption studies, GRS measures the broad bremsstrahlung spectrum in the MeV range born from runaway electrons scattered by impurities as they orbit in the machine. This is used to determine the temporal evolution of the RE distribution function during the current quench, which sheds light on the impact of disruption mitigation techniques on the RE velocity space. Prospects for GRS in deuterium-tritium plasmas include the possibility to infer the energy- and pitch-resolved α particle distribution function from the spectral measurements and using velocity space tomography. This is of special relevance for the forthcoming JET deuterium-tritium campaign - where GRS will be the only diagnostic technique capable to observe α particles - and in view of probing the promises held by the technique for ITER plasmas.

6. Acknowledgments

This work has been carried out within the framework of the EUROfusion Consortium and has received funding from the Euratom research and training programme 2014-2018 and 2019-2020 under grant agreement No 633053. The views and opinions expressed herein do not necessarily reflect those of the European Commission.

References

[1] Massimo Nocente et al. "Neutron spectroscopy measurements of tritium beam transport at JET". In: *Nuclear Fusion* 54.10 (2014), p. 104010.

[2] Z Chen et al. "Simulation of neutron emission spectra from neutral beam-heated plasmas in the EAST tokamak". In: *Nuclear Fusion* 53.6 (2013), p. 063023.

[3] M Schneider et al. "Modelling third harmonic ion cyclotron acceleration of deuterium beams for JET fusion product studies experiments". In: *Nuclear Fusion* 56.11 (2016), p. 112022.

[4] M Nocente et al. "Fast ion energy distribution from third harmonic radio frequency heating measured with a single crystal diamond detector at the Joint European Torus". In: *Review of Scientific Instruments* 86.10 (2015), p. 103501.

[5] M Nocente et al. "Cross section of the d+3He→ α+ p reaction of relevance for fusion plasma applications". In: *Nuclear Fusion* 50.5 (2010), p. 055001.

[6] M Nocente et al. "Gamma-ray emission spectrum from thermonuclear fusion reactions without intrinsic broadening". In: *Nuclear Fusion* 55.12 (2015), p. 123009.

[7] Heinz Knoepfel and DA Spong. "Runaway electrons in toroidal discharges". In: *Nuclear Fusion* 19.6 (1979), p. 785.

[8] Boris N. Breizman et al. "Physics of runaway electrons in tokamaks". In: *Nuclear Fusion* 59.8 (2019), p. 083001.

[9] VG Kiptily et al. "γ-ray diagnostics of energetic ions in JET". In: *Nuclear Fusion* 42.8 (2002), p. 999.

[10] VG Kiptily, FE Cecil, and SS Medley. "Gamma ray diagnostics of high temperature magnetically confined fusion plasmas". In: *Plasma physics and controlled fusion* 48.8 (2006), R59.

[11] Moseev D. et al. "Recent progress for fast-ion diagnostics in magnetically confined plasmas". In: *Reviews of Modern Plasma Physics* 2.7 (2018), p. 1.

[12] DC Pace et al. "Gamma ray imager on the DIII-D tokamak". In: *Review of Scientific Instruments* 87.4 (2016), p. 043507.

[13] Carlos Paz-Soldan et al. "Resolving runaway electron distributions in space, time, and energy". In: *Physics of Plasmas* 25.5 (2018), p. 056105.

[14] M Nocente et al. "Gamma-ray spectroscopy at MHz counting rates with a compact LaBr3 detector and silicon photomultipliers for fusion plasma applications". In: *Review of Scientific Instruments* 87.11 (2016), 11E714.

[15] M Nocente et al. "High Resolution Gamma Ray Spectroscopy at MHz Counting Rates With LaBr _{3} Scintillators for Fusion Plasma Applications". In: *IEEE Transactions on Nuclear Science* 60.2 (2013), pp. 1408–1415.

[16] A Dal Molin et al. "Development of a new compact gamma-ray spectrometer optimised for runaway electron measurements". In: *Review of Scientific Instruments* 89.10 (2018), p. 10I134.

[17] M Nocente et al. "High resolution gamma-ray spectrometer with MHz capabilities for runaway electron studies at ASDEX Upgrade". In: *Review of Scientific Instruments* 89.10 (2018), p. 10I124.

[18] D Rigamonti et al. "The upgraded JET gamma-ray cameras based on high resolution/high count rate compact spectrometers". In: *Review of Scientific Instruments* 89.10 (2018), p. 10I116.

[19] Massimo Nocente et al. "Conceptual design of the radial gamma ray spectrometers system for α particle and runaway electron measurements at ITER". In: *Nuclear Fusion* 57.7 (2017), p. 076016.

[20] M Rebai et al. "Design of gamma-ray spectrometers optimized for fast particle studies at ITER". In: *Review of Scientific Instruments* 89.10 (2018), p. 10I126.

[21] Mirko Salewski et al. "High-definition velocity-space tomography of fast-ion dynamics". In: *Nuclear Fusion* 56.10 (2016), p. 106024.

[22] Massimo Nocente et al. "High-resolution gamma ray spectroscopy measurements of the fast ion energy distribution in JET 4He plasmas". In: *Nuclear Fusion* 52.6 (2012), p. 063009.

[23] MJ Mantsinen et al. "Alpha-Tail Production with Ion-Cyclotron-Resonance Heating of H 4 e-Beam Ions in JET Plasmas". In: *Physical review letters* 88.10 (2002), p. 105002.

[24] Massimo Nocente. "Neutron and gamma-ray emission spectroscopy as fast ion diagnostics in fusion plasmas". PhD thesis. University of Milano-Bicocca, 2012.

[25] Ye O Kazakov et al. "On resonant ICRF absorption in three-ion component plasmas: a new promising tool for fast ion generation". In: *Nuclear Fusion* 55.3 (2015), p. 032001.

[26] Ye O Kazakov et al. "Efficient generation of energetic ions in multi-ion plasmas by radio-frequency heating". In: *Nature Physics* 13.10 (2017), p. 973.

[27] M.J. Mantsinen et al. "Modelling of three-ion ICRF schemes with PION". In: *Proceedings of the 46th EPS conference on plasma physics* (2019).

[28] M Nocente et al. "Energy resolution of gamma-ray spectroscopy of JET plasmas with a LaBr 3 scintillator detector and digital data acquisition". In: *Review of scientific instruments* 81.10 (2010), p. 10D321.

[29] Nocente M. et al. "A quantitative comparison between confined fast ion data and models from radio frequency heating experiments with the three ion scenarios at JET". In: *Proceedings of the 45th EPS conference on plasma physics* (2018).

[30] VG Kiptily et al. "Gamma-ray imaging of D and 4He ions accelerated by ion-cyclotron-resonance heating in JET plasmas". In: *Nuclear Fusion* 45.5 (2005), p. L21.

[31] EM Hollmann et al. "Status of research toward the ITER disruption mitigation system". In: *Physics of Plasmas* 22.2 (2015), p. 021802.

[32] C Paz-Soldan et al. "Recent DIII-D advances in runaway electron measurement and model validation". In: *Nuclear Fusion* 59.6 (2019), p. 066025.

[33] VV Plyusnin et al. "Comparison of runaway electron generation parameters in small, medium-sized and large tokamaks—A survey of experiments in COMPASS, TCV, ASDEX-Upgrade and JET". In: *Nuclear Fusion* 58.1 (2017), p. 016014.

[34] Yaowei Yu et al. "First results on disruption mitigation by massive gas injection in Korea Superconducting Tokamak Advanced Research". In: *Review of Scientific Instruments* 83.12 (2012), p. 123509.

[35] AE Shevelev et al. "Reconstruction of distribution functions of fast ions and runaway electrons in fusion plasmas using gamma-ray spectrometry with applications to ITER". In: *Nuclear Fusion* 53.12 (2013), p. 123004.

[36] E Panontin et al. "Development of Nuclear Radiation Based Tomography Methods for Runaway Electrons in Fusion Plasmas: First Results and Prospects". In: *Proceedings of the 46th EPS conference on plasma physics* (2019).

[37] A Lvovskiy et al. "The role of kinetic instabilities in formation of the runaway electron current after argon injection in DIII-D". In: *Plasma Physics and Controlled Fusion* 60.12 (2018), p. 124003.

[38] VG Kiptily et al. "Gamma-diagnostics of alpha-particles in 4 He and D–T plasmas". In: *Review of scientific instruments* 74.3 (2003), pp. 1753–1756.

[39] M Tardocchi, M Nocente, and G Gorini. "Diagnosis of physical parameters of fast particles in high power fusion plasmas with high resolution neutron and gamma-ray spectroscopy". In: *Plasma Physics and Controlled Fusion* 55.7 (2013), p. 074014.

[40] Mirko Salewski et al. "MeV-range velocity-space tomography from gamma-ray and neutron emission spectrometry measurements at JET". In: *Nuclear Fusion* 57.5 (2017), p. 056001.

[41] Mirko Salewski et al. "On velocity-space sensitivity of fast-ion D-alpha spectroscopy". In: *Plasma Physics and Controlled Fusion* 56.10 (2014), p. 105005.

[42] Asger Schou Jacobsen et al. "Velocity-space sensitivity of neutron spectrometry measurements". In: *Nuclear Fusion* 55.5 (2015), p. 053013.

[43] Mirko Salewski et al. "On velocity space interrogation regions of fast-ion collective Thomson scattering at ITER". In: *Nuclear Fusion* 51.8 (2011), p. 083014.

[44] AS Jacobsen et al. "Velocity-space sensitivities of neutron emission spectrometers at the tokamaks JET and ASDEX Upgrade in deuterium plasmas". In: *Review of Scientific Instruments* 88.7 (2017), p. 073506.

[45] J Galdon-Quiroga et al. "Velocity-space sensitivity and tomography of scintillator-based fast-ion loss detectors". In: *Plasma Physics and Controlled Fusion* 60.10 (2018), p. 105005.

[46] Mirko Salewski et al. "Fast-ion energy resolution by one-step reaction gamma-ray spectrometry". In: *Nuclear Fusion* 56.4 (2016), p. 046009.

[47] Mirko Salewski et al. "Velocity-space observation regions of high-resolution two-step reaction gamma-ray spectroscopy". In: *Nuclear Fusion* 55.9 (2015), p. 093029.

[48] B Madsen et al. "Velocity-space tomography using prior information at MAST". In: *Review of Scientific Instruments* 89.10 (2018), p. 10D125.

[49] M Weiland et al. "Phase-space resolved measurement of 2nd harmonic ion cyclotron heating using FIDA tomography at the ASDEX Upgrade tokamak". In: *Nuclear Fusion* 57.11 (2017), p. 116058.

[50] Jacob Eriksson et al. "Dual sightline measurements of MeV range deuterons with neutron and gamma-ray spectroscopy at JET". In: *Nuclear Fusion* 55.12 (2015), p. 123026.

[51] M Salewski et al. "Alpha-particle velocity-space diagnostic in ITER". In: *Nuclear Fusion* 58.9 (2018), p. 096019.

[52] C Cazzaniga et al. "Response of LaBr3 (Ce) scintillators to 14 MeV fusion neutrons". In: *Nuclear Instruments and Methods in Physics Research Section A: Accelerators, Spectrometers, Detectors and Associated Equipment* 778 (2015), pp. 20–25.

[53] D Rigamonti et al. "Characterization of a compact LaBr3 (Ce) detector with Silicon photomultipliers at high 14 MeV neutron fluxes". In: *Journal of Instrumentation* 12.10 (2017), p. C10007.

[54] Mirko Salewski et al. "Diagnostic of fast-ion energy spectra and densities in magnetized plasmas". In: *Journal of Instrumentation* 14.05 (2019), p. C05019.